Microbial Ecology (2023) 86:2032–2046
https://doi.org/10.1007/s00248-023-02209-7

RESEARCH

The Bacterial Microbiome of the Coral Skeleton Algal Symbiont *Ostreobium* Shows Preferential Associations and Signatures of Phylosymbiosis

B. L. D. Uthpala Pushpakumara[1] · Kshitij Tandon[1] · Anusuya Willis[2] · Heroen Verbruggen[1]

Received: 14 December 2022 / Accepted: 16 March 2023 / Published online: 31 March 2023

Abstract

Ostreobium, the major algal symbiont of the coral skeleton, remains understudied despite extensive research on the coral holobiont. The enclosed nature of the coral skeleton might reduce the dispersal and exposure of residing bacteria to the outside environment, allowing stronger associations with the algae. Here, we describe the bacterial communities associated with cultured strains of 5 *Ostreobium* clades using 16S rRNA sequencing. We shed light on their likely physical associations by comparative analysis of three datasets generated to capture (1) all algae associated bacteria, (2) enriched tightly attached and potential intracellular bacteria, and (3) bacteria in spent media. Our data showed that while some bacteria may be loosely attached, some tend to be tightly attached or potentially intracellular. Although colonised with diverse bacteria, *Ostreobium* preferentially associated with 34 bacterial taxa revealing a core microbiome. These bacteria include known nitrogen cyclers, polysaccharide degraders, sulphate reducers, antimicrobial compound producers, methylotrophs, and vitamin B12 producers. By analysing co-occurrence networks of 16S rRNA datasets from *Porites lutea* and *Paragoniastrea australensis* skeleton samples, we show that the *Ostreobium*-bacterial associations present in the cultures are likely to also occur in their natural environment. Finally, our data show significant congruence between the *Ostreobium* phylogeny and the community composition of its tightly associated microbiome, largely due to the phylosymbiotic signal originating from the core bacterial taxa. This study offers insight into the *Ostreobium* microbiome and reveals preferential associations that warrant further testing from functional and evolutionary perspectives.

Keywords *Ostreobium* · Endolithic algae · Coral holobiont · Coral skeleton · Algal microbiome · Core microbiome · Phylosymbiosis

Introduction

Bacterial interactions with algae are important due to their influence on ecosystem productivity. Through culture-based experiments [1, 2], omics approaches [3, 4], and microbial network studies [5, 6], a range of algal associations with bacteria have been uncovered. The algal phycosphere, an area around the algal cell rich in photosynthetic exudates, is home to diverse bacteria [7, 8] with host interactions that range from mutualistic to parasitic [9, 10]. Organic carbon and inorganic nutrient exchanges are the most common interactions observed between algae and bacteria [11, 12], while more specialised interactions include provision of B vitamins [13, 14], iron chelating siderophores [15], and growth promoting hormones [16] by bacteria.

Tightly associated algal–bacterial systems provide an opportunity to investigate the functional nature and evolutionary basis of algal–bacterial interactions. Phylosymbiosis captures the correlation between the host phylogeny and the relationships of microbial communities associated with those hosts [17]. Both deterministic processes, such as influence on community composition by host traits, and random processes, like changes in microbial community dispersal and host geographical ranges, may lead to phylosymbiosis [18, 19]. Phylosymbiosis has been observed in a number of terrestrial systems [20–22] and is now gaining attention in

✉ B. L. D. Uthpala Pushpakumara
bpushpakumar@student.unimelb.edu.au

[1] School of Biosciences, University of Melbourne, Victoria 3010, Australia

[2] Australian National Algae Culture Collection, CSIRO, Tasmania 7000 Victoria, Australia

marine hosts due to major studies on scleractinian corals [23] and sponges [24] detecting this pattern.

Ostreobium, a siphonous green alga, is an endolithic alga living in marine limestone, and is the principal skeletal alga of corals [25]. *Ostreobium* has also been discovered growing in widely divergent environments such as oyster shells and deep tropical waters. In spite of the divergent environments in which it grows, *Ostreobium* always lives in near darkness [26]. It can also survive in variable concentrations of O_2 and fluctuating pH [26–28]. During bleaching events, *Ostreobium* is shown to provide photosynthates to the coral organism helping to keep it temporarily alive [29, 30]. As an endolithic alga, *Ostreobium* lives in a confined environment with its associated bacteria, which likely reduces the frequency of opportunities for bacterial recruitment or exchange. Such an environment may have resulted in evolutionary pressure to conserve associations and co-disperse. In other confined spaces, such as animal gut, stronger eco-evolutionary patterns have been observed [31].

Extensive work on different biological components associated with corals has been carried out to shed light on the coral holobiont which comprises the coral animal and the associated microorganisms [32]. A large gap remains in our knowledge of microbial associations in the coral skeleton, including with the major skeletal algal symbiont, *Ostreobium*. The aim of this study was to describe the bacterial communities associated with cultured strains from different *Ostreobium* lineages. Using different sample processing protocols, we focus on investigating likely physical associations of bacteria with its algal host. We investigate if *Ostreobium*-bacteria associations present in the cultures are likely to also occur in their natural environment through co-occurrence network analysis. We test whether evolutionary relationships between *Ostreobium* lineages are associated with differences in bacterial community composition, with the prediction that microbial dendrograms built on beta diversity differences would be more congruent with *Ostreobium* phylogeny than expected at random.

Methods

Study Design, Sample Preparation, and DNA Extraction

Cultures of five strains (VRM605, VRM642, VRM644, VRM646, VRM647) representing five clades (P3P14, C, P1K, P4, B3, respectively) of *Ostreobium* were used. Isolation of these strains from skeleton fragments of Great Barrier Reef corals (Heron Island) and molecular identification were described previously [33]. In brief, single algal filaments emerging from the green area of the skeleton (inoculated in culture media) were collected and grown (in modified f/2 media made up of sterile filtered seawater with nutrients as described in [34] and vitamins as described in [35] under 1 µmol m^{-2} s^{-1} photons LED light on a 12 h:12 h light:dark cycle [33]. Phylogenetic affiliations of these strains were determined using chloroplast-encoded *tufA* and *rbcL* markers derived from assembled chloroplast genomes [33]. To investigate likely physical associations, three sample processing protocols were employed which we will call 'whole', 'media", and 'tight'. All sample processing was conducted on the same day. For the 'whole' protocol, *Ostreobium* filaments were collected using wide-bore tip pipettes, placed in sterile centrifuge tubes and snap frozen, thereby characterising all the culture associated bacteria (attached, intracellular and unattached in the culturing media). To generate 'media' dataset, fifty millilitres of spent media from each culture was collected, filtered using 0.22 µm and filters were placed in sterile centrifuge tubes and snap frozen. This data was used to identify unattached and contaminating bacteria. The 'tight' protocol was aimed at characterising potentially intracellular as well as tightly attached bacteria. Algal filaments were washed serially, three times, in sterile modified f/2 media (same modified f/2 media used in microalgal culturing) by vortexing for 15–20 s. The washed algal material was then placed in sterile petri dishes with DNA extraction buffer and the filaments were cut with sterile dissecting scissors allowing the cytoplasmic material to flow out. Finally, the green cytoplasmic content was collected, avoiding the cell wall material as much as possible to enhance the potentially intracellular taxa and snap frozen until processing. All the snap frozen samples were stored at − 20 °C until processing. Although we stored our snap frozen samples at − 20 °C, we thank one of the reviewers for pointing out it is advisable to store samples until processing at − 80 °C to help stabilise the samples by reducing the enzymatic activities even further than they are at − 20 °C. While we added the lysis buffer only to the samples used to generate 'tight' data, it would be advisable to use the same preservation method to prevent differential lysis. To test for contaminant bacteria in the algal growth room, sterile culture media (same modified f/2 media used in microalgal culturing) in a culture flask was maintained with the algal cultures. Negative controls for filter units and media used to wash the algal material were also tested. DNA extractions were performed following [36] with modifications (15 min incubation with 20 mL of 10 mg/mL lysozyme following sample homogenization and 20 s bead beating at 30 Hz with 100 mg of sterile glass beads) described by [37]. Blank DNA extractions were conducted as negative controls.

16S rRNA Gene PCR Amplification, Library Preparation, and Sequencing

Hyper variable regions of the 16S rRNA-gene, V5–V6, were amplified using the primer pairs: 784F [5'- TCGTCGGCA

GCGTCAGATGTGTATAAGAGACAGAGGATTAGATAC CCTGGTA -3'], and 1061R [5'- GTCTCGTGGGCTCGG AGATGTGTATAAGAGACAGCRRCACGAG CTGACG AC-3'] [38] using a 2 step PCR protocol. Illumina adapters that were attached to the primers are shown as underlined. In the first PCR round, each reaction contained 10uL of KAPA HiFi HotStart ReadyMix, 0.5uL of each primer (10uM) and 10uL of DNA template. Previously described PCR conditions [39] were used for 1st and 2nd PCR steps. First-PCR conditions were as follows: 95 °C for 3 min; 25 cycles of 98 °C for 20 s, 60 °C for 15 s, 72 °C for 30 s, a final extension at 72 °C for 1 min. In the second PCR round, each reaction contained 10uL GoTaq Green mix, 0.5uL of each custom-made Illumina index (10uM) and 10uL DNA template. PCR conditions were as follows: 95 °C for 3 min; 24 cycles each at 95 °C for 15 s, 60 °C for 30 s, 72 °C for 30 s, a final extension at 72 °C for 7 min. Triplicate PCRs were conducted for each sample and controls (negative controls for filter unit, media used to wash algal material, algal growth room and DNA extraction blanks). Three PCRs without template DNA were also conducted. A library pool was prepared taking 5uL from each well per plate, cleaned up using beads (80uL beads to 100uL library pool), quality-checked on a TapeStation (model 4200) and sequenced using the Illumina MiSeq platform (2*300 bp paired end reads) at the Walter and Eliza Hall Institute of Medical Research. In total, we sequenced 6 replicates per strain (2 biological replicates * 3 technical replicates) in each protocol.

16S rRNA Gene Analysis in Qiime2

Raw, demultiplexed sequence reads (demultiplexed by the sequence provider (Walter and Eliza Hall Institute of Medical Research) based on the indexing primers used in the 2nd PCR step) were analysed in QIIME2 v2021.2. Cutadapt was used to remove primers [40]. Sequence denoising and chimera checking was performed in DADA2 [41] to correct sequencing errors, low quality bases (–p-trunc-len-f 0, –p-trunc-len-r 0, –p-trim-left-f 0, –p-trim-left-r 0, –p-trunc-q 20), dereplicate and obtain amplicon sequence variants (ASVs). Taxonomy was assigned in QIIME2 against the SILVA database (v132) trained with a naïve Bayes classifier [42, 43]. ASVs identified as mitochondria, chloroplasts, and Archaea were filtered. A phylogenetic tree was constructed using the alignment [44] and phylogeny [45] packages. The filtered table with ASV counts, phylogenetic tree, taxonomy classifications table, and metadata file were used to perform downstream statistical analyses in RStudio.

Statistical Community Analysis

Statistical analyses were performed and graphs produced using R (v4.0.4) [46] using packages phyloseq (v1.32.0) [47], decontam (v1.11.0) [48], microbiome (v1.10.0) [49], vegan (v2.5.7) [50], indicspecies (v1.7.9) [51], and ggplot2 (v3.3.5) [52]. Statistical tests were considered significant at $\alpha = 0.05$ unless otherwise stated. Contaminant ASVs were identified using negative controls (DNA extraction blanks, negative controls for algal growth room, PCR blanks and additionally for the 'media' and 'tight' datasets, negative controls for filter unit and media used to wash algal material were used, respectively) in the R package decontam using default parameters and removed from the respective datasets. Evenly sampled ASV tables created by rarefying to the lowest read number for a given sample (lowest read number in 'whole' = 3247, 'tight' = 14,939, and 'media' = 24,887) were used to calculate metrics of alpha diversity (observed ASVs, Simpson index, Shannon index) and beta diversity (Bray Curtis, Unifrac, weighted-Unifrac). Multivariate homogeneity of group dispersions (PERMDISP) was used to check for the effect of group dispersions on permutational multivariate analysis of variance (PERMANOVA) results. Community structure differences (β-diversity) were statistically compared between 'media' and 'whole', and 'media' and 'tight' using PERMANOVA. Community structure differences between the datasets were visualised with principal coordinate analysis (PCoA). Similarly, alpha diversity data were also analysed to compare the datasets as above by using the non-parametric Kruskal–Wallis test.

An indicator taxa analysis was carried out using indicspecies package to identify bacterial families significantly associated with 'whole', 'tight', and 'media' datasets with 999 permutations to identify taxa that likely represent the loosely attached, tightly attached/intracellular and unassociated/contaminating taxa, respectively. The indicator taxa analysis reports a 'stat' value (point biserial correlation coefficient) which measures the strength of the association of a taxa with a dataset. The 'core' microbiome was calculated to find taxa present among all the strains (detection = 0.001, prevalence = 100/100) in the 'tight' dataset. The 'core' microbiome was calculated at the ASV level and at different taxonomic levels such as phylum and family by aggregating ASVs to the taxonomic level in question. Overall differences in alpha (Kruskal–Wallis test) among the strains were statistically tested for the 'tight' dataset as described above.

To analyse phylosymbiosis, an averaged ASV table was generated from the rarefied ASV table by averaging the ASV abundances by host strains as described elsewhere [53]. From this table, Bray–Curtis, UniFrac, and weighted UniFrac distances were calculated and these beta-diversity matrices were clustered using the UPGMA method (function: hclust(), method = 'average'). Resulting dendrograms were exported in newick format. To generate the host phylogenetic tree, previously published *tuf*A sequences were used [33]. Sequences were aligned using MUSCLE [54] in Geneious Prime v2020.1.2 and a maximum likelihood host

phylogeny built with the IQ-TREE web server with 1000 bootstraps and best-model selection enabled [55]. Host phylogeny and microbial dendrogram were then compared using matching cluster metrics with 10,000 random trees using a previously published Python script [20]. Co-phylogeny plot was created using phytools (v.1.2–0) [56] to compare host and microbial trees.

Co-occurrence Network Analysis on Porites lutea and Paragoniastrea australensis Skeletal Samples

We constructed co-occurrence networks from *P. lutea* and *P. australensis* skeletal samples using a previously published 16S rRNA gene dataset [28] (SRA accession PRJNA753944) to investigate *Ostreobium*-bacteria associations in natural settings and to determine if those associations can be seen in cultured *Ostreobium*. These coral samples were collected from Heron Island (Great Barrier Reef), which is the same study site from which *Ostreobium* strains were isolated by [33]. Bioinformatic analysis was carried out in QIIME2 v2021.2 to obtain ASV tables representing bacterial and chloroplast sequences for each coral species. Any ASV that was present in less than 20% of samples was filtered to remove low prevalent organisms from the correlation analysis. Bacterial taxonomy was assigned using the SILVA database (v132). Chloroplast sequences were reclassified using PhytoRef [57] to identify microalgae in the skeletal samples. Correlation analysis was performed using a previously published shell script [6] in FastSpar [58]. Two individual undirected weighted networks were created using statistically ($p < 0.05$) significant correlations (> 0.5) for each coral species by using the igraph [59] package. Networks were visualised in Cytoscape (version 3.8) [60] and clustered using clusterMaker [61] with the MCL clustering algorithm to identify microbial communities. The Network Analyzer plugin [62] was used to compute global network properties of each network.

Results

Sequencing Overview and Bacterial Microbiome Diversity

To determine likely physical associations, three datasets, 'whole', 'tight', and 'media' were used in this study. We wished to distinguish host associated microbiomes, using 'whole' and 'tight' datasets, from loosely and unassociated microbiomes determined using the 'media' dataset. Sequencing generated 5,526,746 reads across all the algal samples and controls in the "whole' dataset. After removal of contaminants, 446 bacterial ASVs (represented by 858,363 reads) were observed across the 5 *Ostreobium* strains (Supplementary data file). In 'tight' data, sequencing produced 6,619,904 reads across all the algal samples and the controls. After removal of contaminants, 853 ASVs (represented by 1,198,358 reads) were observed across the strains (Supplementary data file). The 'media' dataset generated 5,352,716 reads with an ASV count of 415 (represented by 1,449,465 reads) (Supplementary data file).

Statistically significant community structure differences were evident based on Bray–Curtis distances between 'media' and 'whole' (Fig. 1a) (PERMANOVA $_{\text{mediaVSwhole}} = p = 0.001$, $F_{(1,58)} = 7.49$, $R^2 = 0.11$) as well as 'media' and 'tight' datasets (PERMANOVA $_{\text{mediaVtight}}$ $p = 0.001$, $F_{(1,58)} = 4.94$, $R^2 = 0.08$) (Fig. 1b). Substantially higher ASV richness, evenness and overall Shannon diversity were observed in 'whole' and 'tight' than 'media' data (Fig. 1: c). Overall, 'tight' data showcased the highest overall alpha diversity. All three alpha diversity metrics were significantly different between 'media' and 'whole' data (Kruskal–Wallis test: $\chi^2_{\text{Observed (1)}} = 15.77$, $p = 7.139\text{e-}05$, $\chi^2_{\text{Simpson(1)}} = 21.41$, $p = 3.701\text{e-}06$, $\chi^2_{\text{Shannon(1)}} = 24.09$, $p = 9.181\text{e-}07$) and 'media' and 'tight' data (Kruskal–Wallis test: $\chi^2_{\text{Observed (1)}} = 32.18$, $p = 1.407\text{e-}08$, $\chi^2_{\text{Simpson(1)}} = 39.21$, $p = 3.803\text{e-}10$, $\chi^2_{\text{Shannon(1)}} = 38.46$, $p = 5.602\text{e-}10$).

In support of the beta diversity differences, clear differences in major taxonomic groups were observed between the media dataset and others. The media fraction of each strain consisted almost entirely of *Pseudomonadaceae* (Fig. 2a) accounting for more than 76% of the reads in each strain except VRM642 (45%). This was in stark contrast to the dominant groups for *Ostreobium*-associated datasets (*Methyloligellaceae* in 'whole' data and *Cyclobacteriaceae* in 'tight' data, Fig. 2b and c). These results imply that the unattached microbiome in media is distinct from the bacterial communities in 'whole' and 'tight' datasets.

Taxonomically Diverse Bacterial Associates and an Unexpected Methylotroph Diversity

'Whole' data highlighted all the associated bacteria of *Ostreobium* while 'tight' data provided potential insights into those communities that are tightly attached and intracellular. In 'whole' data, *Proteobacteria* and *Bacteroidetes* were the most dominant phyla accounting for total relative abundance of 64.56% and 22.66%, respectively. The most dominant bacterial family (22.12%) was represented by a methylotrophic bacterium, *Methyloligellaceae* (c_*Alphaproteobacteria*, o_*Rhizobiales*, g_*Methyloceanibacter*) followed by *Rhodobacteraceae* (11.40%), *Saprospiraceae* (10.66%), *Amoebophilaceae* (7.01%), *Rhizobiaceae* (5.23%), and *Marinobacteraceae* (3.55%) (Fig. 2b, Supplementary data).

Of the 25 bacterial phyla detected in the 'tight' data, *Proteobacteria* (57.63%) and *Bacteroidetes* (31.43%) were the most dominant. Ninety different bacterial families were

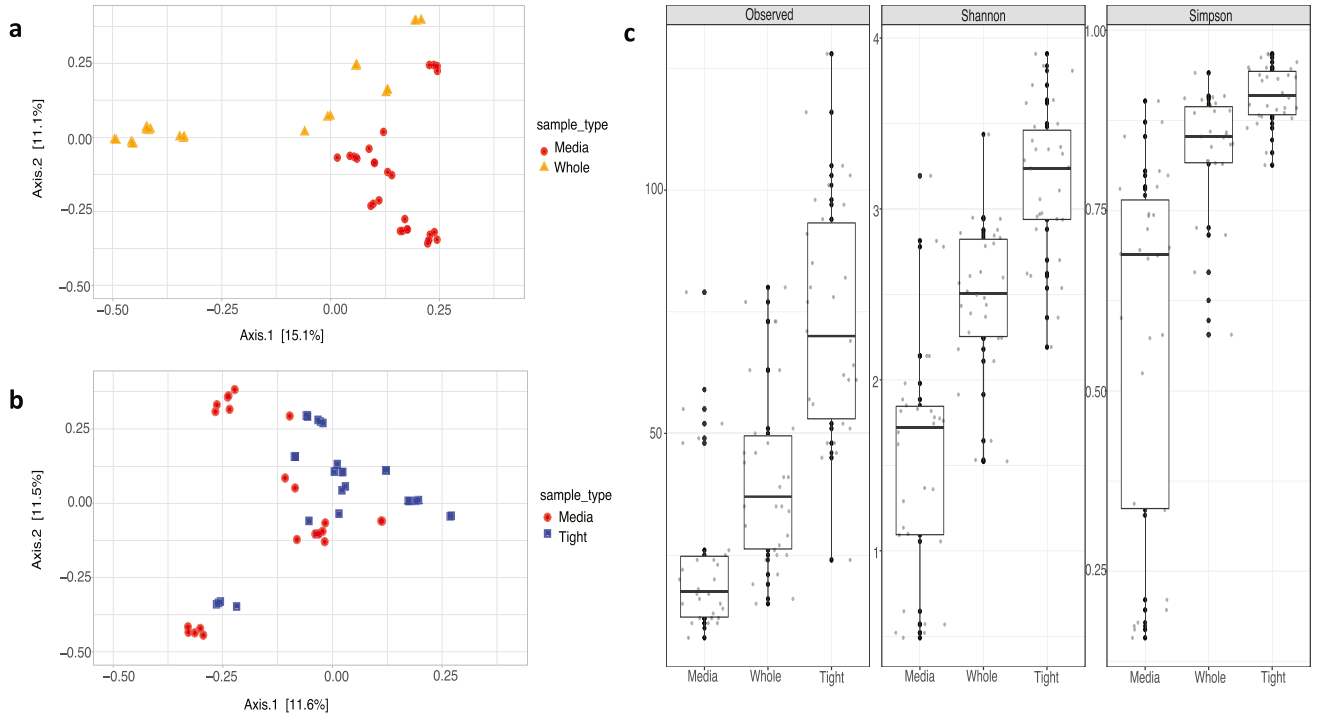

Fig. 1 Principal coordinate analysis and alpha diversity to distinguish datasets. **a** PCoA using Bray–Curtis dissimilarity to distinguish 'media' and 'whole'. **b** PCoA using Bray–Curtis dissimilarity to distinguish 'media' and 'tight'. Coloured dots/triangles/squares represent replicate samples. **c** Alpha diversity differences between the three datasets: observed ASVs indicate richness, Shannon diversity index indicate overall alpha diversity and Simpson diversity index indicate evenness. Black dots represent the replicate samples. Median values are indicated by the horizontal line inside the box

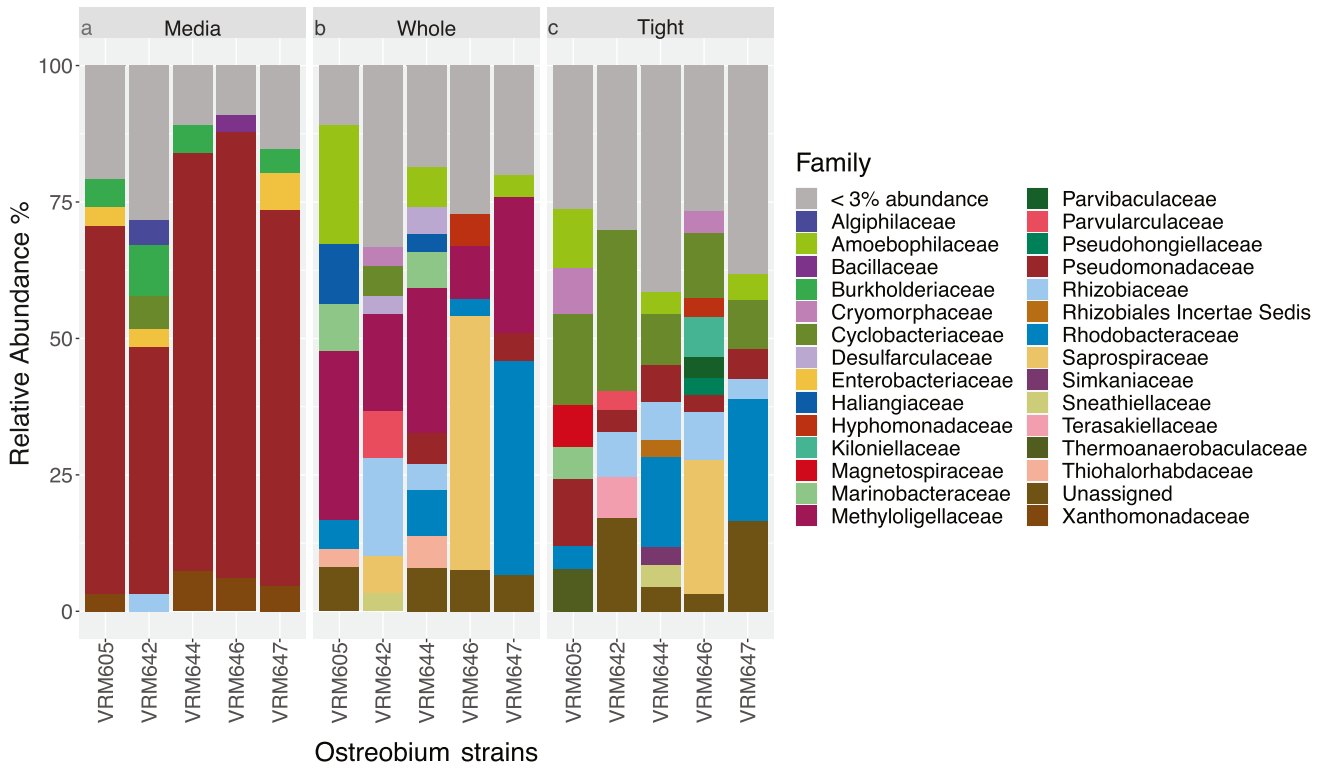

Fig. 2 Bacterial community compositions of the three datasets: relative abundances of major bacterial families found in 'media' (**a**), whole (**b**), and tight (**c**) datasets

associated with *Ostreobium* strains and about 19.60% of the ASVs were taxonomically unidentified at family level. The dataset was dominated by the family *Cyclobacteriaceae* (15.33%) (Fig. 2c) which was only accounting for relative abundance of 2.36% in the 'whole' dataset. *Rhodobacteraceae* (9.56%), *Pseudomonadaceae* (6.34%), and *Rhizobiaceae* (5.70%) were the 2nd, 3rd, and 4th most abundant families. *Cyclobacteriaceae* was represented by genera *Marinoscillum*, *Reichenbachiella*, *Ekhidna*, *Fabibacter*, and *Fulvivirga*.

The most dominant family of the 'whole' dataset, *Methyloligellaceae*, was only contributing to 0.96% of the total relative abundance of the 'tight' dataset. A clear increase in *Pseudomonadaceae* in 'tight' data (6.34%) was observed compared to the 'whole' community (3.03%). The most abundant ASV of the 'tight' data was represented by an uncultured *Alphaproteobacteria* followed by ASVs representing *Pseudomonadaceae* (g_Pseudomonas) and *Rhodobacteraceae* (g_ *Leisingera*). *Chlamydiae*, typically an intracellular taxon, was also an abundant phylum (~ 1.35%) in the 'tight' data while only accounting for 0.27% of the reads in the 'whole' dataset. There was a clear increase in relative abundance of *Kiloniellaceae* (2.28%) in 'tight' compared to 'whole' data (0.74%). In both datasets, *Leisingera* was found to be highly abundant, ranking as the most abundant in the 'tight' dataset as well as the second most abundant in the 'whole' dataset (Supplementary data file).

Since the 'whole' dataset was dominated by a methylotrophic bacterium, both 'whole' and 'tight' datasets were inspected for the presence of other methylotrophs, yielding several other methylotrophic genera such as *OM43* (f_ *Methylophilacea*), *Methylophaga* (f_ *Methylophagaceae*), *Leisingera* (f_ *Rhodobacteraceae*), and *Filomicrobium* (f_*Hyphomicrobiaceae*) [63–65] in varying relative abundances. Among them, *Leisingera* was consistently associated with all strains in both 'whole' and 'tight' datasets.

Closely Associated Bacteria of Ostreobium

The protocol employed in the generation of the 'tight' data provided an opportunity to study an enriched fraction of attached and intracellular bacteria which may be closely associated and possibly influence *Ostreobium* physiology. Alpha diversity as assessed by observed ASV richness, and Simpson and Shannon indices showed that the number of bacterial taxa associated and their evenness were similar among the strains, with none of the differences statistically significant (Kruskal–Wallis test: $\chi^2_{\text{Observed (1)}} = 8.04$, $p = 0.09018$, $\chi^2_{\text{Simpson (1)}} = 8.05$, $p = 0.08986$, $\chi^2_{\text{Shannon (1)}} = 6.85$, $p = 0.1439$).

Ostreobium strains were consistently associated with (that is present in all the 5 strains with a minimum abundance of 0.1%) certain bacterial groups indicating the presence of a core microbiome, with core phyla including *Acidobacteria*, *Actinobacteria*, *Bacteroidetes*, *Gemmatimonadetes*, *PAUC34f*, *Planctomycetes*, *Proteobacteria*, and *Verrucomicrobia*. The core families were represented by 34 bacterial families (including some unassigned at the family level but consistently associated, for example: *Actinomarinales* unassigned at family level) accounting for over 60% of reads in all strains and even > 75% in four out of five strains (Fig. 3). However, at the ASV level, only 6 ASVs (represented by Pseudomonadaceae (2 ASVs), *Marinobacteraceae*, *Sneathiellaceae*, *Rhizobiaceae*, and an *Actinomarinales* unassigned at family level) were consistently associated among all the strains averaging for ~ 10% of the total reads. This implies that although *Ostreobium* associates with conserved bacterial families their members are different at a finer taxonomic level possibly representing different species or strains. This was also clear from the presence/absence of the ASVs representing the 34 core families across the strains (Table S1). These findings imply that different members of the core bacterial families are hosted by different *Ostreobium* strains, resulting in differences in community structure.

Next, we attempted to determine the likely physical associations through an indicator taxa analysis by identifying which taxa preferentially associate with each dataset (Table S2). We expected the loosely attached communities to decrease in abundance following the serial washing step. Therefore, the indicators of 'tight' data could be thought of as those that are potentially tightly attached or intracellular as it is expected for the loosely attached communities to decrease in abundance following the serial washing step. Likewise, indicators of 'whole' data could be thought of as those that are loosely attached. Among the 38 bacterial taxa detected as indicators of 'tight' fraction, *Cyclobacteriacea* (stat = 0.59, $p = 0.001$) and members of candidate phylum PAUC34f (stat = 0.61, $p = 0.001$) were identified as the most strongly associated. Both these groups represent the core taxa of *Ostreobium* we defined earlier in the core microbiome analysis. Other than these two, 15 more core bacterial families such as *Pseudohongiellaceae*, *Alphaprotoeobacteria* unassigned at family level, *Rhodothermaceae*, *Pedosphaeraceae*, *Kiloniellaceae*, *Gemmatimonadaceae*, *bacteriap25*, *Rhizobiales Incertae Sedis*, *Terasakiellaceae*, *Magnetospiraceae*, *Parvibaculaceae*, *Phycisphaeracea*, *Gammaproteobacteria* unassigned at family level, *Gammaptoteobacteria Ga0077536* and *Flavobacteriales* unassigned at family level were also found as indicators of the 'tight' data. *Methyloligellaceae*, another core taxon (stat = 0.88, $p = 0.001$) was the most strongly associated family of the 'whole' data out of the 13 indicator taxa. Indicators of the 'whole' data also represented 5 more core bacterial families such as *Actinomarinales* unassigned at family level, *Microtrichaceae*, *Mitrotichales* unassigned at family level, *Haliangiaceae* and *Desulfarculaceae.* The indicator taxa analysis

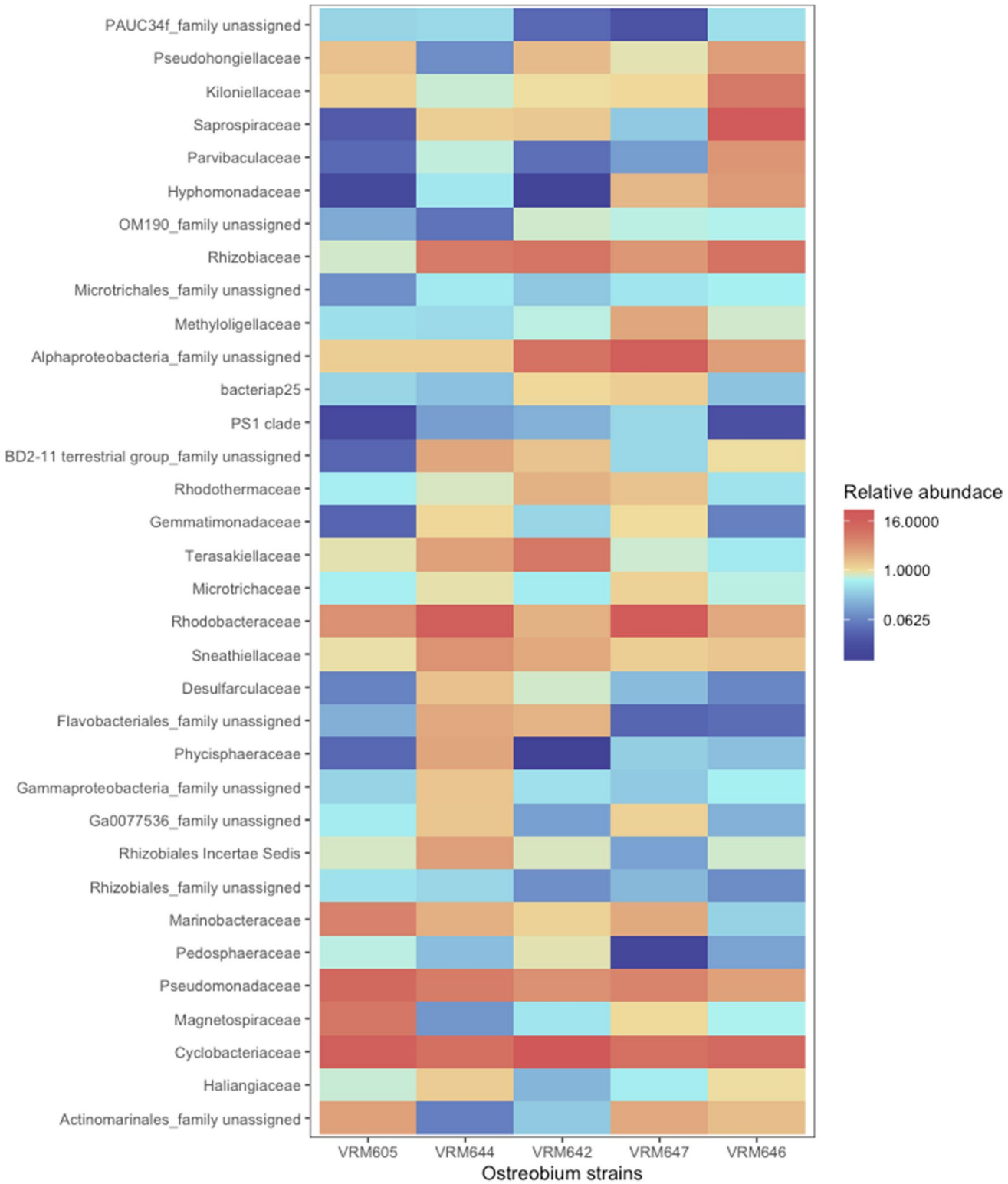

Fig. 3 Heat map of the core bacterial families: The relative abundance of the 34 core bacterial families detected using the 'tight' data across different strains

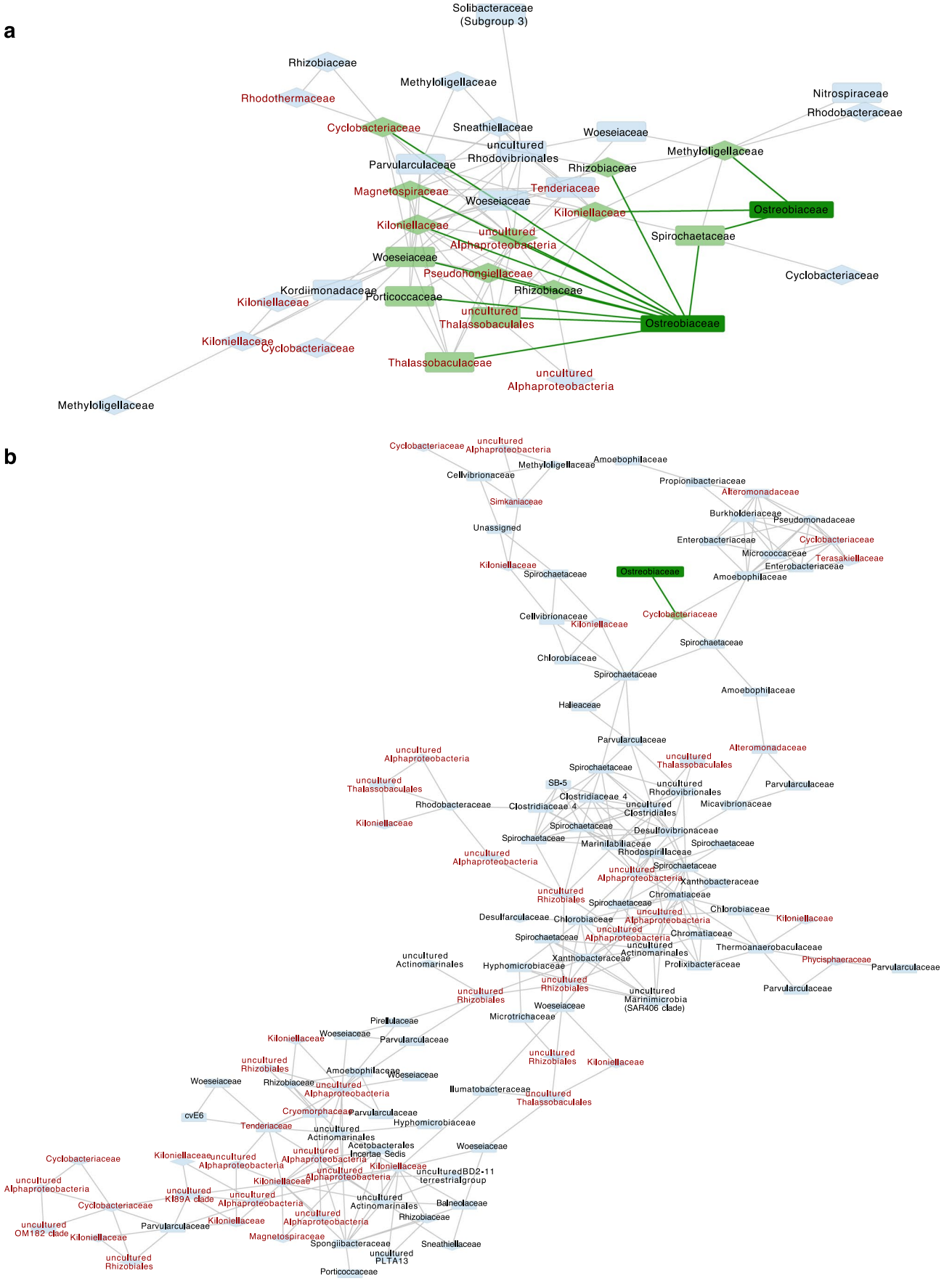
a
Solibacteraceae (Subgroup 3)
Rhizobiaceae
Methyloligellaceae
Rhodothermaceae
Nitrospiraceae
Rhodobacteraceae
Cyclobacteriaceae
Sneathiellaceae
Woeseiaceae
uncultured Rhodovibrionales
Methyloligellaceae
Parvularculaceae
Rhizobiaceae
Magnetospiraceae
Tenderiaceae
Woeseiaceae
Kiloniellaceae
Ostreobiaceae
Kiloniellaceae
uncultured Alphaproteobacteria
Spirochaetaceae
Woeseiaceae
Pseudohongiellaceae
Cyclobacteriaceae
Kordiimonadaceae
Rhizobiaceae
Kiloniellaceae
Porticoccaceae
uncultured Thalassobaculales
Ostreobiaceae
Kiloniellaceae
Cyclobacteriaceae
Thalassobaculaceae
uncultured Alphaproteobacteria
Methyloligellaceae
b
Cyclobacteriaceae
uncultured Alphaproteobacteria
Amoebophilaceae
Methyloligellaceae
Cellvibrionaceae
Propionibacteriaceae
Alteromonadaceae
Simkaniaceae
Burkholderiaceae
Pseudomonadaceae
Unassigned
Enterobacteriaceae
Cyclobacteriaceae
Micrococcaceae
Terasakiellaceae
Kiloniellaceae
Spirochaetaceae
Ostreobiaceae
Enterobacteriaceae
Amoebophilaceae
Cellvibrionaceae
Cyclobacteriaceae
Kiloniellaceae
Spirochaetaceae
Chlorobiaceae
Spirochaetaceae
Amoebophilaceae
Halieaceae
Parvularculaceae
Alteromonadaceae
uncultured Alphaproteobacteria
uncultured Thalassobaculales
Spirochaetaceae
uncultured Thalassobaculales
SB-5
uncultured Rhodovibrionales
Parvularculaceae
Clostridiaceae 4
Rhodobacteraceae
Clostridiaceae 4
uncultured Clostridiales
Micavibrionaceae
Kiloniellaceae
Spirochaetaceae
Spirochaetaceae
Desulfovibrionaceae
Marinilabiliaceae
Spirochaetaceae
uncultured Alphaproteobacteria
Rhodospirillaceae
Spirochaetaceae
uncultured Alphaproteobacteria
Xanthobacteraceae
uncultured Rhizobiales
Chromatiaceae
Spirochaetaceae
Chlorobiaceae
Desulfarculaceae
Chlorobiaceae
uncultured Alphaproteobacteria
Kiloniellaceae
Spirochaetaceae
uncultured Alphaproteobacteria
Chromatiaceae
uncultured Actinomarinales
Thermoanaerobaculaceae
uncultured Actinomarinales
Xanthobacteraceae
Hyphomicrobiaceae
Prolixibacteraceae
Phycisphaeraceae
Parvularculaceae
uncultured Rhizobiales
uncultured Rhizobiales
uncultured Marinimicrobia (SAR406 clade)
Parvularculaceae
Woeseiaceae
Microtrichaceae
Pirellulaceae
Woeseiaceae
Kiloniellaceae
Parvularculaceae
uncultured Rhizobiales
Kiloniellaceae
Amoebophilaceae
Woeseiaceae
Woeseiaceae
Rhizobiaceae
uncultured Alphaproteobacteria
Ilumatobacteraceae
uncultured Thalassobaculales
cvE6
Cryomorphaceae
Parvularculaceae
Hyphomicrobiaceae
Tenderiaceae
uncultured Actinomarinales
Acetobacterales
Incertae Sedis
Woeseiaceae
Cyclobacteriaceae
Kiloniellaceae
uncultured Alphaproteobacteria
uncultured Alphaproteobacteria
Kiloniellaceae
uncultured Alphaproteobacteria
uncultured Kl89A clade
uncultured Alphaproteobacteria
uncultured Actinomarinales
Balneolaceae
Cyclobacteriaceae
uncultured Alphaproteobacteria
Kiloniellaceae
Rhizobiaceae
uncultured OM182 clade
Parvularculaceae
Magnetospiraceae
Kiloniellaceae
Spongiibacteraceae
Sneathiellaceae
uncultured PLTA13
uncultured Rhizobiales
Porticoccaceae

◂**Fig. 4** Co-occurrence network analysis of *Paragoniastrea australensis* and *Porites lutea* skeletal samples: *Ostreobium*-bacteria module from *P. australensis* (**a**) and *P. lutea* (**b**). Diamond shape nodes indicate core bacterial families of 'tight' data. Taxa labelled in red represent those that were found as indicators of 'tight' data. Direct edges from *Ostreobium* nodes are colored in green. Edge width is continuously mapped to edge weight

also found 14 taxa (table S2) associated with both the 'tight' and 'whole' dataset. These taxa also represented core bacteria taxa such as *Saprospiraceae*, *Gemmatimonadetes* unclassified at family level, *OM190* unclassified at family level, *Hyphomonadaceae*, *Rhizobiaceae*, *Rhodobacteraceae*, *Sneathiellaceae*, and *Marinobacteraceae*. These taxa could also be thought as those that are potentially tightly attached or intracellular. In total, 31 core bacterial taxa were found as indicators of either 'tight', 'whole', or 'tight and whole'. These results indicate that the majority of the core taxa of *Ostreobium* may have an attached lifestyle. *Pseudomonadaceae* (stat = 0.89, $p = 0.001$) was the most strongly associated family of the 'media' data.

Culture-Based Associations Are Observed in the Co-occurrence Networks of Ostreobium and Bacteria

The co-occurrence network created using *P. lutea* skeletal samples consisted of 138 nodes and 322 edges while the *P. australensis* co-occurrence network consisted of 85 nodes and 209 edges. The global network properties for each network can be found in Supplementary table S3. By clustering, we identified one *Ostreobium*-bacterial module from *P. lutea* and one from *P. australensis* (Fig. 4a and b). The *P. australensis* module consisted of 2 representative *Ostreobium* ASVs annotated as *Ostreobiaceae*. This module included 35 nodes and 104 edges (Fig. 4a). The *P. lutea* module consisted of 1 representative *Ostreobium* ASV (annotated as *Ostreobiaceae*) and included 126 nodes and 310 edges (Fig. 4b). Both *Ostreobium*-bacteria modules showed high clustering coefficients (> 0.5) indicating densely connected neighbourhoods.

The most important observation was that the majority of bacterial communities potentially interacting with *Ostreobium* in the natural environment represented most of the core bacterial families (Fig. 4: diamond shaped nodes) and indicator taxa of 'tight' data (Fig. 4: taxa labelled in red). For instance, in *P. australensis*, representative *Ostreobium* nodes showed significant co-occurrences with many *Cyclobacteriaceae* and *Kiloniellaceae* (Fig. 4a) which were found to be both core and indicator taxa of the 'tight' data. In *P. lutea,* the representative *Ostreobium* node was connected to the rest of the community via *Cyclobacteriaceae* (Fig. 4b) highlighting possible tight association with this bacterial lineage.

Ostreobium Phylogeny Correlates with Bacterial Community Structure

A significant difference in community structures among strains led us to investigate patterns of phylosymbiosis. We first quantified the phylosymbiotic signal using the 'whole' dataset representing all the culture-associated bacteria and found no statistically significant congruence between the trees (normalized matching cluster score (nMC) = 0.60, $p = 0.8755$ for all Bray–Curtis, Unifrac, and weighted Unifrac UPGMA comparisons with the host tree). For the 'tight' data, on the other hand, topological congruence analysis showed a significant ($p = 0.0272$) association between the host phylogenetic tree and microbial dendrogram constructed on Bray–Curtis distances, with a nMC score of 0.30 (Fig. 5 and Table 1). Matching cluster method considers sections of subtree congruence to weigh the topological congruency of the trees and reports a nMC score [66]. Normalized matching cluster scores closer to zero indicate higher topological congruence and reveal signatures of phylosymbiosis. With over 60% of reads in each strain stemming from ASVs representing core bacterial families (see above), we investigated whether they were responsible for the significant signal observed, and we detected the same significant nMC of 0.30 for the core microbial Bray–Curtis distances. Although core weighted and unweighted UniFrac distances generated non-significant results, more evidence for phylosymbiosis was apparent based on improved p values compared to the previous analysis on the entire community (Table 1).

Discussion

Despite extensive work on the coral holobiont, many questions about the major algal symbiont of coral skeleton, *Ostreobium*, remain to be answered. Understanding how the major algal symbiont of the coral interacts with the surrounding microbiome helps to extend our knowledge on the coral holobiont. As a first step towards understanding these interactions, we describe the bacterial microbiome of *Ostreobium* using diverse clades of cultured *Ostreobium*. This study led to the identification of taxa that were likely to be intracellular or closely attached, which can be used to guide future studies to confirm their location. Our study revealed that *Ostreobium* consistently associates with 34 bacterial families constituting the majority of its microbiome. However, these bacterial families are represented by distinct ASVs that lead to community differences between the strains. We identified phylosymbiotic signatures stemming from these core bacterial families implying that they may preferentially associate or co-differentiate with *Ostreobium* hosts. By constructing co-occurrence networks on coral skeletal samples, we show that the culture-based associations inferred in this study exist

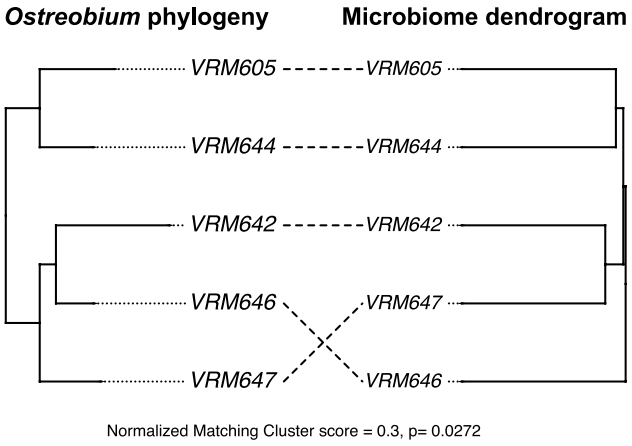

Fig. 5 Topological congruence between the host phylogeny and microbial dendrogram: Host phylogenetic tree was constructed using *tufA* sequences. The microbiome tree represents the UPGMA tree constructed on Bray–Curtis distances. This was built using the ASVs representing the core bacterial families of the 'tight' data. The normalised matching cluster score (nMC) and p value indicates significant congruence. VRM605, VRM642, VRM644, VRM646, and VRM647 represent the *Ostreobium* strains

was shown to be potentially involved in symbiosis with the eukaryotes in the skeleton through a metagenomic analysis [71]. To the best of our knowledge, there's no known *Chlamydiae* infecting or found associated with algae [72, 73]. However, it is believed that *Chlamydiae* played an important role in the evolution of photoautotrophic eukaryotes (the ménage-à-trois hypothesis) [74]. Cell-associated microbial aggregates containing *Chlamydiae* and *Endozoicomonas* are present in coral tips [75] and deserve further study. Moreover, consistent with observations from Ricci et al. [39] on coral skeletal samples, we also found an ASV assigned to an uncultured bacterium from phylum *Actinobacteria* representing class *Acidimicrobiia* in all the *Ostreobium* strains.

Our three-dataset study design allowed distinguishing the host associated microbiome from the taxa in the media fractions and investigating their likely physical associations. The media fractions of each strain were less diverse, almost entirely composed of *Pseudomonadaceae* and were significantly different in composition from the host associated data. Although our data do not constitute proof of physical associations, they shed light on likely locations of particular

Table 1 Summary of Phylosymbiosis testing: 'Testing type' highlights different tests carried out using the 'tight' data**.** Normalised matching score ranges from 0 (complete congruence) to 1 (complete incongruence). Significant results are in bold text

Testing type	Distance metric	Normalized matching cluster score	*p* value
Entire community	**Bray**	**0.3**	**0.0272**
Entire community	Unifrac	0.6	0.8687
Entire community	Weighted-Unifrac	0.6	0.8764
Core (ASVs representing core bacterial families)	**Bray**	**0.3**	**0.0272**
Core (ASVs representing core bacterial families)	Unifrac	0.4	0.1657
Core (ASVs representing core bacterial families)	Weighted-Unifrac	0.4	0.1687

in natural settings and the taxa we identified as potentially closely associated frequently co-occur with *Ostreobium*.

The *Ostreobium* microbiome included bacteria that have been previously found in coral skeleton microbiomes. Bacteria representing *Candidatus Amoebophilus*, *Kiloniellaceae, Rhizobiales*, and *Myxococcales* were recently shown to be preferentially associated with the coral skeleton microbiome [67]. We detected these bacterial taxa in high abundance in *Ostreobium* cultures, suggesting that their presence in the coral skeleton may be due to an association with *Ostreobium*. The *Cyclobacteriacea*, previously identified as consistently associated, understudied or new taxa in the coral microbiome [67], was here shown to be a potentially tightly attached and perhaps even intracellular bacterium of *Ostreobium*. In addition to these, the microbiome found in our study was dominated by bacterial phyla predominantly found in coral skeletons, such as *Proteobacteria*, *Bacteroidetes*, *Actinobacteria*, *Planctomycetes*, and *Acidobacteria* [68–70]. We also found a significant abundance of *Chlamydia* which

bacterial groups. In generating our 'tight' data, our approach was to wash away most of the loosely attached and contaminating bacteria through serial washing, enriching tightly associated bacteria. We cut open the filaments and collected the cytoplasmic material to further enrich intracellular bacteria. Unexpectedly, the 'tight' data showed the highest richness. This may be attributed to the methodology we used for data generation. It is likely that cutting open the filaments has revealed bacteria that were not detected in the 'whole' dataset due to being present at low abundance compared to the loosely attached bacteria and those found in the media. While none of these methods confirm the nature of physical association, they do show trends reflecting which bacteria are more likely to be tightly associated with their host.

Comparison between 'tight' with 'whole' data allowed identifying taxa that are more likely to be intracellular or tightly attached. The *Methyloligellaceae*, a very abundant bacterial family in the 'whole' dataset, was significantly

reduced in the 'tight' dataset, suggesting that the serial washing may have largely removed these taxa, which we could therefore speculate to be loosely attached to the host algal cell wall. Both the taxonomic composition analysis and indicator taxa showed *Cyclobacteriacea* to be significantly associated with the 'tight' data implying they may be closely attached or potentially intracellular. *Cyclobacteriaceae* are known to degrade polysaccharides which could contribute to the carbon metabolism of the coral holobiont [76]. Moreover, they are involved in carotenoid biosynthesis, antibiotic resistance, and quorum-sensing, all of which can benefit the alga [76]. *PAU34f*, a candidate phylum known for its symbiotic associations of sponges, was also found to be significantly more prevalent in the 'tight' dataset. Genomic studies have revealed that they have the potential to degrade both sponge and algae derived carbohydrates, presumably provide phosphate reservoirs to the sponge host in deprivation periods, produce antimicrobial compounds that can be used by the host as a defence strategy and harbour signatures of host associations (eukaryotic-like proteins) in the genome [77]. Presence of eukaryotic-like proteins may help mediate interactions with the algal host and the degradation of algal derived carbohydrates can provide *Ostreobium* with remineralised inorganic nutrients.

Our results show that *Ostreobium* is colonised by a core set of bacterial families that differ on a finer taxonomic scale, resulting in differences in the community structure among strains. By studying these core bacterial taxa, we identified key functional types associated with *Ostreobium*. Most of the bacteria represented known nitrogen cyclers (*Rhizobiaceae*, *Terasakiellaceae*, *Kiloniellaceae*, *Sneathiellaceae* [78–81], sulphate reducers (*Desulfarculaceae* [82], polysaccharide degraders (*Cyclobacteriaceae*, *PAUC34f*, *Pseudohongiellaceae* [76, 77, 83], and antimicrobial compound producers (*Cyclobacteriaceae*, *Myxococcales* (families *bacteriap25* and *Haliangiaceae* [76, 84–86]). Apart from these, we also found potential vitamin B12 producers such *Rhodobacteraceae* (*Roseobacter* clade) which are known mutualists of eukaryotes [1, 87]. *Ostreobium*'s dependence on bacteria for vitamin B12 was previously shown, and it was hypothesised based on metatranscriptomic data of the coral holobiont that *Rhodobacteraceae* may provide this vitamin [88]. Members of *Rhizobiaceae* are nitrogen fixers, and this metabolism has also been documented in *Terasakiellaceae* [78]. Both *Kiloniellaceae* and *Sneathiellaceae* are potential denitrifiers involved in reduction of nitrates to gaseous nitrogen [79, 81]. *Kiloniellaceae* were previously shown to be closely associated with *Symbiodiniaceae* [89] and a preferential coloniser of the coral skeleton [67]. Our results and previous studies therefore suggest that *Kiloniellaceae* may be an important associate of both algal symbionts of the tissue and skeleton. Nitrogen fixation can benefit the alga by providing an organic nitrogen source and also the coral holobiont, which lives in an oligotrophic environment by contributing to the nitrogen budget [90]. The presence of both nitrogen fixers and denitrifiers shows that the *Ostreobium*-associated microbiome may contribute to nitrogen homeostasis, contributing to the stabilisation of the coral holobiont. Moreover, our indicator analysis revealed a range of bacterial taxa as indicators of 'tight' data, in addition to *Cyclobacteriaceae* and *PAU34f*. In total, out of the 34 core bacterial families, 31 of them were either indicators of 'tight', 'whole', or 'tight and whole'. With regard to the physical location of the core microbiome, these results suggest that the majority of the core bacteria live attached (tightly or loosely) to or potentially inside the *Ostreobium* filaments rather than floating in the media. Additional work should be carried out to confirm these associations through 3-dimensional imaging.

The associations of *Ostreobium* with a range of methylotrophic bacteria are intriguing. Methylotrophs can utilise reduced carbon substrates without carbon–carbon bonds (i.e., C1 substrates) as their source of carbon and energy [64]. Methanotrophs, the methylotrophs that can utilise the potent greenhouse gas methanol, are of special interest with regard to climate change [91]. While we detected diverse methylotrophs such as *OM43* (family *Methylophilaceae*), *Methylophaga* (family *Methylophagaceae*), and *Filomicrobium* (family *Hyphomicrobiaceae*) in the microbiome, the genus *Methyloceanibacter* of family *Methyloligellaceae* and *Leisingera* of family *Rhodobacteraceae* were the most dominant and consistently associated. Members of the family *Methyloligellaceae* have been shown to utilise both methylated compounds and methane as their carbon source [92]. *Leisingera*, represent organisms that can grow by oxidation of methyl groups and specifically *L.methylohalidivorans* use methyl halides as the sole source of carbon and energy [93, 94]. Interestingly, *Leisingera* species have also been shown to produce antimicrobial compounds and secondary metabolites such as siderophores and acyl-homoserine lactones involved with quorum sensing that may aid in symbiotic relationships [95]. The fact that methylotrophs are commonly isolated from macroalgae [96] suggests unsuspected algae-methylotroph associations. Considering the diversity and consistent association of some methylotrophs with *Ostreobium*, our results suggest a possible production of methanol and/or methylated compounds by *Ostreobium*. Recently, methylotrophic genus *Methylobacterium* was identified as an intracellular core genus of *Symbiodiniaceae* [89]. These findings suggest possible intricate relationships between methylotrophs and algal symbionts of the coral organism. A relationship that may be similar to terrestrial plants and methylotrophs where these bacteria affect the overall health of the holobiont by producing plant growth hormones [97]. Overall, *Ostreobium*-associated methylotrophs may play an important role in C1 metabolism of the

holobiont that involves energy metabolism as well as nutrient cycling.

Our co-occurrence network analysis revealed two *Ostreobium*-bacteria modules from both coral species, *P. lutea* and *P. australensis*. Network modules are thought to represent biologically meaningful microbial communities [98]. Bacterial taxa in both these modules represented most of the core bacterial families and indicators of 'tight' data. As described earlier, we proposed these core and indicator taxa as the closely associated microbiome of *Ostreobium* that may be potentially influencing the *Ostreobium* physiology. Co-occurrence results suggest that *Ostreobium* tends to maintain these important associations even in cultures. These significant co-occurrences help to further support our hypothesis. Overall, we demonstrated that cultured *Ostreobium* harbours bacteria that have been previously described in coral skeleton microbiomes and those that co-occur significantly in the natural coral environment. These results show that culture-associated microbiota represents associations present in their natural environment.

Dissimilarity in microbial community structure among the host lineages led us to quantify the correlation between the host phylogeny and bacterial community composition to look for patterns of phylosymbiosis. We quantified the phylosymbiotic signal from both 'whole' and 'tight' data to investigate how the signal differs between the two. Our results indicated that the signal from all the culture-associated bacteria in 'whole' were insignificant. While phylosymbioses involve trends across the entire microbiome composition, their absence does not rule out that bacteria preferentially associate with certain species of hosts or co-differentiate with them [99]. By analysing the closely associated microbiome using the 'tight' dataset, we found that the microbial dendrograms built on the entire community composition as well as the ASVs representing the core bacterial families produce the same significant results highlighting the origination of the phylosymbiotic signal. Consequently, we hypothesise that *Ostreobium* preferentially associates with these core bacterial taxa and some of these bacteria may be evolutionarily conserved. A recent study provided evidence for the presence of patterns of phylosymbiosis in microbiomes of coral reef invertebrates including sponges, corals, octocorals, and ascidians [100]. Another study found varying strengths of phylosymbiotic signals among different Australian coral compartments (tissue, mucus, and skeleton), with endolithic communities providing the strongest signal [23]. These studies together with results from our work show the prevalence of phylosymbiosis in coral compartments and their associated microeukaryotes.

Overall, we provide a comprehensive study on the microbiome of the major coral skeleton symbiont *Ostreobium* and shed light on phylosymbiotic signatures of an algal–bacterial system. Our results indicate preferential associations between certain bacterial taxa and *Ostreobium* which warrants further testing of these associations both from functional and evolutionary perspectives. Based on the known functions of these bacterial taxa, *Ostreobium*-bacteria associations are likely to play important roles in providing access to various nutrients and maintaining homeostasis (such as nitrogen balance) in the coral organism. Bacterial symbioses play key roles in eukaryote's ability to adapt to changing environmental conditions [101, 102]. If this is true for *Ostreobium*, these associations may help *Ostreobium* to live in the coral skeleton which is an extreme environment for an alga. Future studies may shed light on how bacteria affect *Ostreobium* health and its role in adapting to environmental changes, as well as the effect of *Ostreobium*-bacteria associations on coral bleaching. In conclusion, our findings extend the knowledge on the microbiome of endolithic algae, coral holobiont, and coral reef microbial ecology and enhance our understanding of evolutionary relationships between microalgae and bacteria.

Supplementary Information The online version contains supplementary material available at https://doi.org/10.1007/s00248-023-02209-7.

Acknowledgements We are grateful for Stephen Wilcox from the Walter and Eliza Hall Institute of Medical Research for his assistance in library sequencing. We thank Dr. Francessco Ricci for providing raw QIIME2 files linked to Bioproject PRJNA753944 and Dr. Cintia Iha for providing valuable help in Bioinformatic analysis.

Author Contribution UP, HV, AW, and KT designed the research. UP performed DNA extraction, library preparation, and bioinformatic analyses. UP wrote the first draft of the manuscript. All authors contributed to the final edited version of the manuscript.

Funding Open Access funding enabled and organized by CAUL and its Member Institutions We acknowledge the funding from the Australian Research Council grant DP200101613, Melbourne Research Scholarship and the ResearchPlus Postgraduate Top-Up Scholarship Grants Program and National Research Collections Australia, CSIRO.

Data availability Sequence data are available under NCBI BioProject ID PRJNA910678.

Declarations

Competing Interests The authors declare no competing interests.

References

1. Cooper MB et al (2019) Cross-exchange of B-vitamins underpins a mutualistic interaction between *Ostreococcus tauri* and *Dinoroseobacter shibae*. ISME J. https://doi.org/10.1038/s41396-018-0274-y
2. Bunbury F et al (2022) Exploring the onset of B12-based mutualisms using a recently evolved *Chlamydomonas* auxotroph and B12-producing bacteria. Environ Microbiol 24:3134–3147. https://doi.org/10.1111/1462-2920.16035
3. Krohn-Molt I et al (2013) Metagenome survey of a multispecies and alga-associated biofilm revealed key elements of bacterial-algal interactions in photobioreactors. Appl Environ Microbiol. https://doi.org/10.1128/AEM.01641-13
4. Ramanan R et al (2015) Phycosphere bacterial diversity in green algae reveals an apparent similarity across habitats. Algal Res. https://doi.org/10.1016/j.algal.2015.02.003
5. Milici M et al (2016) Co-occurrence analysis of microbial taxa in the Atlantic ocean reveals high connectivity in the free-living bacterioplankton. Front Microbiol 7(MAY):1–20. https://doi.org/10.3389/fmicb.2016.00649
6. Pushpakumara BLDU, Tandon K, Willis A, Verbruggen H (2023) Unravelling microalgal-bacterial interactions in aquatic ecosystems through 16S rRNA gene-based co-occurrence networks. Sci Rep. https://doi.org/10.1038/s41598-023-27816-9
7. Bell W, Mitchell R (1972) Chemotactic and growth responses of marine bacteria to algal extracellular products. Biol Bull. https://doi.org/10.2307/1540052
8. Seymour JR, Amin SA, Raina JB, Stocker R (2017) Zooming in on the phycosphere: the ecological interface for phytoplankton-bacteria relationships. Nat Microbiol. https://doi.org/10.1038/nmicrobiol.2017.65
9. Mayali X, Azam F (2004) Algicidal bacteria in the sea and their impact on algal blooms. J Eukaryot Microbiol. https://doi.org/10.1111/j.1550-7408.2004.tb00538.x
10. Bagwell CE et al (2016) Discovery of bioactive metabolites in biofuel microalgae that offer protection against predatory bacteria. Front Microbiol. https://doi.org/10.3389/fmicb.2016.00516
11. J. J. Cole, "Interactions between bacteria and algae in aquatic ecosystems.," Annu Rev Ecol Syst *Vol. 13*, 1982, https://doi.org/10.1146/annurev.es.13.110182.001451.
12. A. Buchan, G. R. LeCleir, C. A. Gulvik, and J. M. González, "Master recyclers: features and functions of bacteria associated with phytoplankton blooms.," *Nature reviews. Microbiology*. 2014, https://doi.org/10.1038/nrmicro3326.
13. Croft MT, Lawrence AD, Raux-Deery E, Warren MJ, Smith AG (2005) Algae acquire vitamin B12 through a symbiotic relationship with bacteria. Nature. https://doi.org/10.1038/nature04056
14. Kazamia E et al (2012) Mutualistic interactions between vitamin B12-dependent algae and heterotrophic bacteria exhibit regulation. Environ Microbiol. https://doi.org/10.1111/j.1462-2920.2012.02733.x
15. Amin SA, Green DH, Hart MC, Küpper FC, Sunda WG, Carrano CJ (2009) Photolysis of iron-siderophore chelates promotes bacterial-algal mutualism. Proc Natl Acad Sci U S A. https://doi.org/10.1073/pnas.0905512106
16. Seyedsayamdost MR, Case RJ, Kolter R, Clardy J (2011) The Jekyll-and-Hyde chemistry of *phaeobacter gallaeciensis*. Nat Chem. https://doi.org/10.1038/nchem.1002
17. Lim SJ, Bordenstein SR (1922) An introduction to phylosymbiosis. Proc R Soc B Biol Sci 287:2020. https://doi.org/10.1098/rspb.2019.2900
18. Moeller AH, Suzuki TA, Lin D, Lacey EA, Wasser SK, Nachman MW (2017) Dispersal limitation promotes the diversification of the mammalian gut microbiota. Proc Natl Acad Sci USA. https://doi.org/10.1073/pnas.1700122114
19. F. Mazel, K. M. Davis, A. Loudon, W. K. Kwong, M. Groussin, and L. W. Parfrey, "Is host filtering the main driver of phylosymbiosis across the tree of life?," *mSystems*, vol. 3, no. 5, pp. 1–15, 2018, https://doi.org/10.1128/msystems.00097-18.
20. A. W. Brooks, K. D. Kohl, R. M. Brucker, E. J. van Opstal, and S. R. Bordenstein, "Phylosymbiosis: relationships and functional effects of microbial communities across host evolutionary history," *PLoS Biol.*, vol. 14, no. 11, 2016, https://doi.org/10.1371/journal.pbio.2000225.
21. R. E. Ley *et al.*, "Evolution of mammals and their gut microbes," *Science (80-.).*, 2008, https://doi.org/10.1126/science.1155725.
22. Yeoh YK et al (2017) Evolutionary conservation of a core root microbiome across plant phyla along a tropical soil chronosequence. Nat Commun. https://doi.org/10.1038/s41467-017-00262-8
23. Pollock FJ et al (2018) Coral-associated bacteria demonstrate phylosymbiosis and cophylogeny. Nat Commun 9(1):1–13. https://doi.org/10.1038/s41467-018-07275-x
24. Thomas T et al (2016) Diversity, structure and convergent evolution of the global sponge microbiome. Nat Commun. https://doi.org/10.1038/ncomms11870
25. Tandon K et al (2022) Every refuge has its price: *Ostreobium* as a model for understanding how algae can live in rock and stay in business. Semin Cell Dev Biol. https://doi.org/10.1016/j.semcdb.2022.03.010
26. Verbruggen H, Tribollet A (2011) Boring algae. Curr Biol. https://doi.org/10.1016/j.cub.2011.09.014
27. Magnusson SH, Fine M, Kühl M (2007) Light microclimate of endolithic phototrophs in the scleractinian corals *Montipora monasteriata* and *Porites cylindrica*. Mar Ecol Prog Ser. https://doi.org/10.3354/meps332119
28. F. Ricci *et al.*, "Fine-scale mapping of physicochemical and microbial landscapes clarifies the spatial structure of the coral skeleton microbiome," *ResearchSquare*, pp. 1–16, 2022, https://doi.org/10.21203/rs.3.rs-1735748.
29. Fine M, Loya Y (2002) Endolithic algae: an alternative source of photoassimilates during coral bleaching. Proc R Soc B Biol Sci. https://doi.org/10.1098/rspb.2002.1983
30. C. T. Galindo-Martínez *et al.*, "The role of the endolithic alga *Ostreobium* spp. during coral bleaching recovery," *Sci. Rep.*, 2022, https://doi.org/10.1038/s41598-022-07017-6.
31. Kohl KD, Varner J, Wilkening JL, Dearing MD (2018) Gut microbial communities of American pikas (*Ochotona princeps*): evidence for phylosymbiosis and adaptations to novel diets. J Anim Ecol. https://doi.org/10.1111/1365-2656.12692
32. Rohwer F, Seguritan V, Azam F, Knowlton N (2002) Diversity and distribution of coral-associated bacteria. Mar Ecol Prog Ser. https://doi.org/10.3354/meps243001
33. Pasella MM, Lee M-FE, Marcelino VR, Willis A, Verbruggen H (2022) Ten *Ostreobium* (Ulvophyceae) strains from Great Barrier Reef corals as a resource for algal endolith biology and genomics. Phycologia 61(4):452–458. https://doi.org/10.1080/00318884.2022.2064132
34. R. R. GUILLARD and J. H. RYTHER, "Studies of marine planktonic diatoms. I. *Cyclotella nana Hustedt,* and *Detonula confervacea (cleve) Gran.*," *Can. J. Microbiol.*, 1962, https://doi.org/10.1139/m62-029.
35. R. R. L. Guillard, "Culture of phytoplankton for feeding marine invertebrates," in *Culture of Marine Invertebrate Animals*, 1975.
36. Wilson K et al (2002) Genetic mapping of the black tiger shrimp *Penaeus monodon* with amplified fragment length polymorphism. Aquaculture 204(3–4):297–309. https://doi.org/10.1016/S0044-8486(01)00842-0

37. L. M. Hartman, M. J. H. van Oppen, and L. L. Blackall, "Microbiota characterization of *Exaiptasia diaphana* from the Great Barrier Reef," *Anim. Microbiome*, vol. 2, no. 1, 2020, https://doi.org/10.1186/s42523-020-00029-5.
38. Andersson AF, Lindberg M, Jakobsson H, Bäckhed F, Nyrén P, Engstrand L (2008) Comparative analysis of human gut microbiota by barcoded pyrosequencing. PLoS ONE. https://doi.org/10.1371/journal.pone.0002836
39. Ricci F, Fordyce A, Leggat W, Blackall LL, Ainsworth T, Verbruggen H (2021) Multiple techniques point to oxygenic phototrophs dominating the *Isopora palifera* skeletal microbiome. Coral Reefs 40(2):275–282. https://doi.org/10.1007/s00338-021-02068-z
40. M. Martin, "Cutadapt removes adapter sequences from high-throughput sequencing reads," *EMBnet.journal*, 2011, https://doi.org/10.14806/ej.17.1.200.
41. Callahan BJ, McMurdie PJ, Rosen MJ, Han AW, Johnson AJA, Holmes SP (2016) DADA2: high-resolution sample inference from Illumina amplicon data. Nat Methods. https://doi.org/10.1038/nmeth.3869
42. F. Pedregosa *et al.*, "Scikit-learn: machine learning in Python," *J. Mach. Learn. Res.*, 2011.
43. Bokulich NA et al (2018) Optimizing taxonomic classification of marker-gene amplicon sequences with QIIME 2's q2-feature-classifier plugin. Microbiome. https://doi.org/10.1186/s40168-018-0470-z
44. Katoh K, Standley DM (2013) MAFFT multiple sequence alignment software version 7: improvements in performance and usability. Mol Biol Evol. https://doi.org/10.1093/molbev/mst010
45. Price MN, Dehal PS, Arkin AP (2010) FastTree 2 - approximately maximum-likelihood trees for large alignments. PLoS ONE. https://doi.org/10.1371/journal.pone.0009490
46. R Core Team, "R core team (2021)," *R: A language and environment for statistical computing. R Foundation for Statistical Computing, Vienna, Austria. URL* http://www.R-project.org.
47. McMurdie PJ, Holmes S (2013) Phyloseq: an R Package for reproducible interactive analysis and graphics of microbiome census data. PLoS ONE. https://doi.org/10.1371/journal.pone.0061217
48. N. M. Davis, Di. M. Proctor, S. P. Holmes, D. A. Relman, and B. J. Callahan, "Simple statistical identification and removal of contaminant sequences in marker-gene and metagenomics data," *Microbiome*, 2018, https://doi.org/10.1186/s40168-018-0605-2.
49. L. Lahti, S. Shetty, and T. Blake, "Tools for microbiome analysis in R," *Microbiome Package Version 0.99*. 2017.
50. J. Oksanen *et al.*, "Package 'vegan' title community ecology package Version 2.5–7," *R*, 2020.
51. De Cáceres M, Legendre P, Moretti M (2010) Improving indicator species analysis by combining groups of sites. Oikos. https://doi.org/10.1111/j.1600-0706.2010.18334.x
52. H. Wickhan, "ggplot2: elegant graphics for data analysis hadley," *J. Stat. Softw.*, 2009.
53. Trevelline BK, Sosa J, Hartup BK, Kohl KD (1923) A bird's-eye view of phylosymbiosis: weak signatures of phylosymbiosis among all 15 species of cranes. Proceedings Biol Sci 287:2020. https://doi.org/10.1098/rspb.2019.2988
54. Edgar RC (2004) MUSCLE: multiple sequence alignment with high accuracy and high throughput. Nucleic Acids Res. https://doi.org/10.1093/nar/gkh340
55. Minh BQ et al (2020) IQ-TREE 2: new models and efficient methods for phylogenetic inference in the genomic era. Mol Biol Evol. https://doi.org/10.1093/molbev/msaa015
56. Revell LJ (2012) phytools: an R package for phylogenetic comparative biology (and other things). Methods Ecol Evol. https://doi.org/10.1111/j.2041-210X.2011.00169.x
57. Decelle J et al (2015) PhytoREF: a reference database of the plastidial 16S rRNA gene of photosynthetic eukaryotes with curated taxonomy. Mol Ecol Resour 15(6):1435–1445. https://doi.org/10.1111/1755-0998.12401
58. Watts SC, Ritchie SC, Inouye M, Holt KE (2019) FastSpar: rapid and scalable correlation estimation for compositional data. Bioinformatics 35(6):1064–1066. https://doi.org/10.1093/bioinformatics/bty734
59. T. Csardi, G., & Nepusz, "The igraph software package for complex network research. InterJournal, Complex Systems.," *igraph Softw. Packag.*, 2006.
60. Shannon P et al (2003) Cytoscape: a software environment for integrated models of biomolecular interaction networks. Genome Res. https://doi.org/10.1101/gr.1239303
61. Morris JH et al (2011) ClusterMaker: a multi-algorithm clustering plugin for Cytoscape. BMC Bioinformatics. https://doi.org/10.1186/1471-2105-12-436
62. Assenov Y, Ramírez F, Schelhorn SESE, Lengauer T, Albrecht M (2008) Computing topological parameters of biological networks. Bioinformatics. https://doi.org/10.1093/bioinformatics/btm554
63. J. K. Schaefer, K. D. Goodwin, I. R. McDonald, J. C. Murrell, and R. S. Oremland, "*Leisingera methylohalidivorans gen. nov., sp. nov.*, a marine methylotroph that grows on methyl bromide," *Int. J. Syst. Evol. Microbiol.*, 2002, https://doi.org/10.1099/ijs.0.01960-0.
64. Chistoserdova L (2015) Methylotrophs in natural habitats: current insights through metagenomics. Appl Microbiol Biotechnol. https://doi.org/10.1007/s00253-015-6713-z
65. Henriques AC, De Marco P (2015) Complete genome sequences of two strains of 'Candidatus Filomicrobium marinum', a methanesulfonate-degrading species. Genome Announc. https://doi.org/10.1128/genomeA.00160-15
66. Bogdanowicz D, Giaro K (2013) On a matching distance between rooted phylogenetic trees. Int J Appl Math Comput Sci. https://doi.org/10.2478/amcs-2013-0050
67. F. Ricci, K. Tandon, J. R. Black, K.-A. Lê Cao, L. L. Blackall, and H. Verbruggen, "Host traits and phylogeny contribute to shaping coral-bacterial symbioses," *mSystems*, vol. 7, no. 2, 2022, https://doi.org/10.1128/msystems.00044-22.
68. Fine M, Roff G, Ainsworth TD, Hoegh-Guldberg O (2006) Phototrophic microendoliths bloom during coral 'white syndrome.' Coral Reefs. https://doi.org/10.1007/s00338-006-0143-4
69. Sweet MJ, Croquer A, Bythell JC (2011) Bacterial assemblages differ between compartments within the coral holobiont. Coral Reefs. https://doi.org/10.1007/s00338-010-0695-1
70. Li J, Chen Q, Long LJ, De Dong J, Yang J, Zhang S (2014) Bacterial dynamics within the mucus, tissue and skeleton of the coral *Porites lutea* during different seasons. Sci Rep. https://doi.org/10.1038/srep07320
71. K. Tandon *et al.*, "Genomic view of the diversity and functional role of archaea and bacteria in the skeleton of the reef-building corals *Porites lutea* and *Isopora palifera*," *Gigascience*, pp. 1–12, 2022, https://doi.org/10.1093/gigascience/giac127.
72. Becker B, Hoef-Emden K, Melkonian M (2008) Chlamydial genes shed light on the evolution of photoautotrophic eukaryotes. BMC Evol Biol. https://doi.org/10.1186/1471-2148-8-203
73. Collingro A, Köstlbacher S, Horn M (2020) Chlamydiae in the environment. Trends Microbiol. https://doi.org/10.1016/j.tim.2020.05.020
74. Ball SG et al (2013) Metabolic effectors secreted by bacterial pathogens: essential facilitators of plastid endosymbiosis? Plant Cell. https://doi.org/10.1105/tpc.112.101329
75. J. Maire *et al.*, "*Endozoicomonas-chlamydiae* interactions in cell-associated microbial aggregates of the coral," *bioRxiv*, 2022, https://doi.org/10.1101/2022.11.28.517745.

76. Pinnaka AK, Tanuku NRS (2014) "The family cyclobacteriaceae", The Prokaryotes: Other Major Lineages of Bacteria and The. Archaea. https://doi.org/10.1007/978-3-642-38954-2_139
77. Astudillo-García C, Slaby BM, Waite DW, Bayer K, Hentschel U, Taylor MW (2018) Phylogeny and genomics of SAUL, an enigmatic bacterial lineage frequently associated with marine sponges. Environ Microbiol. https://doi.org/10.1111/1462-2920.13965
78. J. M. Tiedje, "Ecology of denitrification and dissimilatory nitrate reduction to ammonium," *Environ. Microbiol. Anaerobes*, 1988.
79. M. Kurahashi, Y. Fukunaga, S. Harayama, and A. Yokota, "*Sneathiella glossodoripedis sp. nov*., a marine alphaproteobacterium isolated from the nudibranch *Glossodoris cincta*, and proposal of Sneathiellales ord. nov. and Sneathiellaceae fam. nov," *Int. J. Syst. Evol. Microbiol.*, 2008, https://doi.org/10.1099/ijs.0.65328-0.
80. L. M. Carrareto Alves, J. A. M. De Souza, A. D. M. Varani, and E. G. D. M. Lemos, "The family Rhizobiaceae," in *The Prokaryotes: Alphaproteobacteria and Betaproteobacteria*, 2014, https://doi.org/10.1007/978-3-642-30197-1_297.
81. Imhoff JF, Wiese J (2014) The order Kiloniellales. The Prokaryotes: Alphaproteobacteria and Betaproteobacteria. https://doi.org/10.1007/978-3-642-30197-1_301
82. Kuever J (2014) The family desulfarculaceae. The Prokaryotes: Deltaproteobacteria and Epsilonproteobacteria. https://doi.org/10.1007/978-3-642-39044-9_270
83. Francis B, Urich T, Mikolasch A, Teeling H, Amann R (2021) North Sea spring bloom-associated Gammaproteobacteria fill diverse heterotrophic niches. Environ Microbiomes. https://doi.org/10.1186/s40793-021-00385-y
84. S. M. Rosales, M. W. Miller, D. E. Williams, N. Traylor-Knowles, B. Young, and X. M. Serrano, "Microbiome differences in disease-resistant vs. susceptible Acropora corals subjected to disease challenge assays," *Sci. Rep.*, 2019, https://doi.org/10.1038/s41598-019-54855-y.
85. Wrótniak-Drzewiecka W, Brzezińska AJ, Dahm H, Ingle AP, Rai M (2016) Current trends in myxobacteria research. Annals of Microbiology. https://doi.org/10.1007/s13213-015-1104-3
86. Ludington WB et al (2017) Assessing biosynthetic potential of agricultural groundwater through metagenomic sequencing: a diverse anammox community dominates nitrate-rich groundwater. PLoS ONE. https://doi.org/10.1371/journal.pone.0174930
87. Ramanan R, Kim BH, Cho DH, Oh HM, Kim HS (2016) Algae-bacteria interactions: evolution, ecology and emerging applications. Biotechnol Adv. https://doi.org/10.1016/j.biotechadv.2015.12.003
88. Iha C et al (2021) Genomic adaptations to an endolithic lifestyle in the coral-associated alga Ostreobium. Curr Biol 31(7):1393-1402.e5. https://doi.org/10.1016/j.cub.2021.01.018
89. Maire J et al (2021) Intracellular bacteria are common and taxonomically diverse in cultured and in hospite algal endosymbionts of coral reefs. ISME J 15(7):2028–2042. https://doi.org/10.1038/s41396-021-00902-4
90. Rädecker N, Pogoreutz C, Voolstra CR, Wiedenmann J, Wild C (2015) Nitrogen cycling in corals: The key to understanding holobiont functioning? Trends Microbiol. https://doi.org/10.1016/j.tim.2015.03.008
91. Jiang H et al (2010) Methanotrophs: multifunctional bacteria with promising applications in environmental bioengineering. Biochem Eng J. https://doi.org/10.1016/j.bej.2010.01.003
92. Takeuchi M et al (2019) Possible cross-feeding pathway of facultative methylotroph Methyloceanibacter caenitepidi Gela4 on methanotroph Methylocaldum marinum S8. PLoS ONE. https://doi.org/10.1371/journal.pone.0213535
93. H. Schäfer, "Isolation of Methylophaga spp. from marine dimethylsulfide-degrading enrichment cultures and identification of polypeptides induced during growth on dimethylsulfide," *Appl. Environ. Microbiol.*, 2007, https://doi.org/10.1128/AEM.02074-06.
94. T. Martens, T. Heidorn, R. Pukal, M. Simon, B. J. Tindall, and T. Brinkhoff, "Reclassification of *Roseobacter gallaeciensis* Ruiz-Ponte et al. 1998 as *Phaeobacter gallaeciensis gen. nov., comb. nov*., description of *Phaeobacter inhibens sp. nov.*, reclassification of *Ruegeria algicola* (Lafay et al. 1995) Uchino et al. 1999 as Marinovu," *Int. J. Syst. Evol. Microbiol.*, 2006, https://doi.org/10.1099/ijs.0.63724-0.
95. S. M. Gromek *et al.*, "Leisingera sp. JC1, a bacterial isolate from hawaiian bobtail squid eggs, produces indigoidine and differentially inhibits vibrios," *Front. Microbiol.*, 2016, https://doi.org/10.3389/fmicb.2016.01342.
96. M. Janvier, C. Frehel, F. Grimont, and F. Gasser, "*Methylophaga marina gen. nov*., *sp. nov*. and *Methylophaga thalassica sp. nov.*, marine methylotrophs," *Int. J. Syst. Bacteriol.*, 1985, https://doi.org/10.1099/00207713-35-2-131.
97. Omer ZS, Tombolini R, Broberg A, Gerhardson B (2004) Indole-3-acetic acid production by pink-pigmented facultative methylotrophic bacteria. Plant Growth Regul. https://doi.org/10.1023/B:GROW.0000038360.09079.ad
98. Chun SJ, Cui Y, Lee JJ, Choi IC, Oh HM, Ahn CY (2020) Network analysis reveals succession of Microcystis genotypes accompanying distinctive microbial modules with recurrent patterns. Water Res. https://doi.org/10.1016/j.watres.2019.115326
99. Boscaro V et al (2022) Microbiomes of microscopic marine invertebrates do not reveal signatures of phylosymbiosis do not reveal signatures of phylosymbiosis. Nat Microbiol. https://doi.org/10.1038/s41564-022-01125-9
100. O'Brien PA et al (2020) Diverse coral reef invertebrates exhibit patterns of phylosymbiosis. ISME J. https://doi.org/10.1038/s41396-020-0671-x
101. Bosch TCG, McFall-Ngai MJ (2011) Metaorganisms as the new frontier. Zoology. https://doi.org/10.1016/j.zool.2011.04.001
102. McFall-Ngai M et al (2013) Animals in a bacterial world, a new imperative for the life sciences. Proc Natl Acad Sci USA. https://doi.org/10.1073/pnas.1218525110